THE JOURNAL OF PHYSICAL CHEMISTRY Letters

pubs.acs.org/JPCL

Vibrational Microspectroscopy of Single Proteins

Satoru Fujiyoshi,*,† Yo Furuya,† Mineo Iseki,† Masakatsu Watanabe,†,§ and Michio Matsushita*,†

†Department of Physics, Tokyo Institute of Technology, Tokyo, 152-8551, Japan, †Center for Promotion of Integrated Science, and §School of Advanced Sciences, Graduate University for Advanced Studies, Kanagawa, 240-0193, Japan

ABSTRACT Vibrational infrared absorption of a single protein molecule was detected at a few kelvins as infrared-induced recovery of visible fluorescence of a dye with which the protein was labeled. This sensitive method of detecting infrared absorption was demonstrated for a single bovine serum albumin (BSA) molecule labeled with Alexa Fluor 660 by determining the vibrational infrared absorption spectrum of the backbone vibrations of the α-helical structure in the wavelength region around 6 μm (1650 cm^{-1}). In addition to measuring the vibrational infrared absorption spectrum, the visible fluorescence can be simultaneously used for imaging of the same dye-labeled single protein molecules.

SECTION Kinetics, Spectroscopy

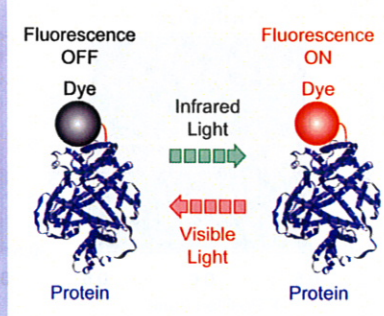

Single-molecule imaging using visible fluorescence[1,2] of dye-labeled proteins has been established to reveal in situ location of single proteins.[3−5] Biological processes would be unraveled truly at a single-molecule level if structural information was obtained on the same proteins. Single-molecule spectroscopy using visible fluorescence has brought new information on the structure and the dynamics of proteins, which was inaccessible by other methods.[6−11] Information on the 3D structure of the backbone of individual proteins would be provided if vibrational infrared-absorption spectroscopy[12−15] was applied to single proteins. However, detection of infrared absorption of a backbone vibration of a single protein has not yet been achieved. We report here that vibrational infrared absorption spectroscopy can be performed on a single protein at a temperature of a few kelvins by measuring infrared-induced recovery of visible fluorescence of a dye with which the protein was labeled. When continuously irradiated by a visible laser light, visible-fluorescent dyes, in general, will end up completely nonfluorescent, even at a few kelvins.[16,17] We found a dye that when used as a fluorescence label of a protein recovers fluorescence by infrared irradiation of the dye-labeled protein. It turned out that the fluorescence recovery was caused by infrared vibrational absorption of the labeled protein. Owing to the response to the infrared that works only at a few kelvins, this dye serves as an epi-molecular probe of the infrared absorption of a single protein. It was crucial for a sample immersed in superfluid helium to develop a new optical setup that allows superposing the diffraction-limited focus of infrared laser light on that of visible laser light.

Figure 1a shows the optical setup developed for single-protein vibrational microspectroscopy. The light source for the visible was the output of a He−Ne laser at a wavelength of 633 nm, and that for the infrared was the output of a quantum-cascade laser tunable from 1570 to 1670 cm^{-1} in wavenumber (6.0 to 6.4 μm in wavelength). The collimated visible and infrared laser lights were collinearly combined at the dichroic mirror (DM). To avoid the chromatic aberration between the visible and the infrared wavelengths, we used reflecting optics for the objective lens and all other elements in the path common to the two laser lights. The scanning of the foci of the two laser lights in the sample was accomplished from outside the cryostat by tilting the motorized flat mirror under a condition of the telecentric arrangement of a pair of concave mirrors (focal length f of 500 mm).[17] The beam paths were purged with dry air to eliminate infrared absorption due to ambient water vapor. Because the sample was immersed in superfluid helium, the 3D field distribution of the two laser lights in the sample was measured around an extra focus on plane A indicated in Figure 1a. Figure 1b shows the focus adjusted onto plane A of the infrared laser light (left) and that of the visible laser light (right). The coincidence of the two foci on plane A guarantees the spatial coincidence of the foci on a common focal plane in the sample in superfluid helium.

The objective lens (f of 4 mm and numerical aperture of 0.6) is used in superfluid helium and works for the visible as well as the infrared wavelengths. The lens basically follows the reflecting objective developed for low-temperature ultraviolet and visible microspectroscopy,[17−19] except that in the present work, calcium fluoride (CaF_2) was chosen as a material that transmits both visible and infrared lights. Because of its crystal structure, polishing optical surfaces on CaF_2 was extremely demanding. Because of imperfection of the optical surfaces of the objective lens, the fluorescence image of a single molecule shown in Figure 2a deviated from the ideal diffraction image

Received Date: June 23, 2010
Accepted Date: August 5, 2010

DOI: 10.1021/jz100858b | J. Phys. Chem. Lett. 2010, 1, 2541–2545

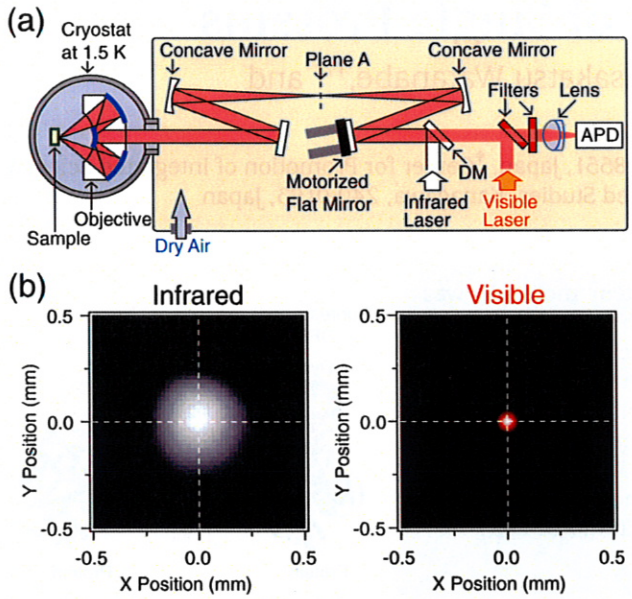

Figure 1. (a) Visible and infrared two-color laser-scanning confocal microscope developed for vibrational microspectroscopy of single proteins at a few kelvins. The visible laser light was used in linear polarization, whereas the infrared light was in circular polarization. APD stands for an avalanche photodiode. (b) Focal image taken at plane A of the infrared laser light (left) and that of the visible laser light (right). The coincidence of the two foci on plane A guarantees that the two lasers were focused at the same position of a single protein in superfluid helium.

of a point source, which is a disk surrounded by concentric rings.[19] The central disk remained as the bright disk with a diffraction-limited size, but the innermost concentric ring broke up into a couple of weaker spots. Despite the surface imperfection, the objective is free from chromatic aberration in the wavelength region throughout from the visible to the infrared. A sample area of at least $(100\ \mu m)^2$ can be properly imaged with both of the visible and the infrared foci overlapping.[19]

The protein studied was bovine serum albumin (BSA). It was labeled with a fluorescent dye, Alexa Fluor 660 carboxylic acid succinimidyl ester (A660) (Molecular Probes, the chemical formula of which is not open to the public), which formed a chemical bond with the NH_2 group of lysine or arginine residues of BSA. The condition for the labeling reaction was adjusted such that in the resultant sample the ratio of the amount of the total BSA to the bound A660 was 1:1. After finishing the reaction, >99% of the dyes not bound to BSA were removed by a desalting spin column. A deuterium oxide (D_2O) solution of A660-labeled BSA was prepared at a concentration of 10^{-11} M with 20 mM phosphate buffer (pH 7) in the presence of 1 % wt/wt polyvinyl alcohol. D_2O was used as a solvent to avoid infrared absorption by H_2O in the wavelength region we measured. The solution was spin-coated on a CaF_2 substrate with 3000 rpm for 60 s. A660 absorbs the visible laser light at 633 nm and fluoresces with the emission maximum at 690 nm. BSA has an infrared absorption band due to in total 582 C=O backbone stretching vibrations.[20] This vibrational band is called amide I, the wavenumber of which is sensitive to the secondary structure of the protein.

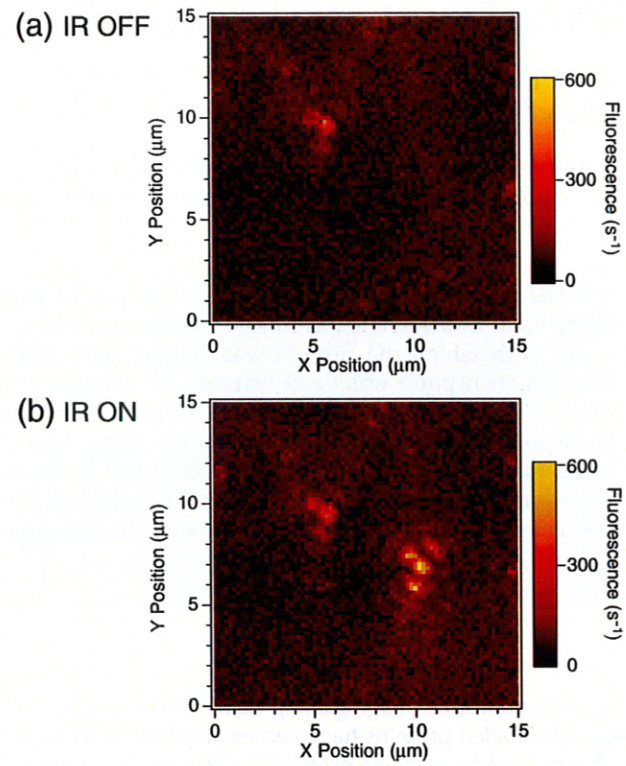

Figure 2. (a) Visible-fluorescence image of a thin film containing spatially isolated single A660-labeled BSA molecules at 1.5 K. (b) Image subsequently taken for the same area with additional infrared irradiation. The intensity of the visible I_{VIS} was 60 W cm^{-2}, and the additional infrared was at a wavenumber ν_{IR} of 1650 cm^{-1} with the intensity of the infrared I_{IR} of 3000 W cm^{-2}.

The absorption maximum of BSA is at 1650 cm^{-1}, corresponding to rich content of α-helices in the protein.

Figure 2a,b shows the visible fluorescence image of the same area of a spin-coated thin film containing A660-labeled BSA molecules at a temperature of 1.5 K. The image shown in Figure 2a was taken with visible irradiation alone, whereas the one in Figure 2b was subsequently taken with simultaneous visible and infrared irradiation. The infrared wavenumber ν_{IR} was fixed at 1650 cm^{-1}, the absorption maximum of the amide I band of BSA. The sample solution used for the film was dilute enough to give spatially isolated fluorescence spots of single A660-labeled BSA molecules in the image.[17] In the sample area imaged Figure 2a,b, two A660-labeled BSA molecules can be located at $x = 6\ \mu m$ and $y = 10\ \mu m$ and at $x = 10\ \mu m$ and $y = 7\ \mu m$. They are different in response to the infrared irradiation.

The additional infrared irradiation at 1.5 K caused a drastic effect on the single A660-labeled BSA molecule at $x = 10\ \mu m$ and $y = 7\ \mu m$ in the images of Figure 2a,b. This molecule did not fluoresce at all under visible irradiation alone (Figure 2a), whereas it fluoresced markedly when infrared irradiation was added (Figure 2b). In contrast, infrared irradiation had no effect on the A660-labeled BSA molecule at $x = 6\ \mu m$ and $y = 10\ \mu m$. It continued to fluoresce in the same way when the infrared irradiation was added (Figure 2b). When visible irradiation was continued, this molecule and all other A660-labeled BSA molecules ended up nonfluorescent at a few

DOI: 10.1021/jz100858b | J. Phys. Chem. Lett. 2010, 1, 2541–2545

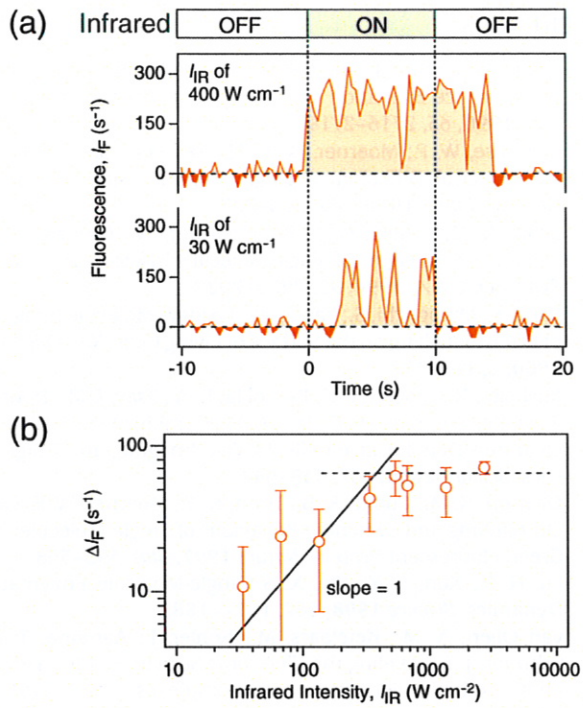

Figure 3. (a) Time courses of visible-fluorescence intensity of a single A660-labeled BSA molecule taken with a time resolution of 0.3 s at 1.5 K. The sample was continuously irradiated with the visible, whereas infrared irradiation was applied for 10 s with I_{IR} of 30 W cm^{-2} in the lower trace and 400 W cm^{-2} in the upper trace. (b) Dependence of the infrared-induced fluorescence recovery ΔI_F on I_{IR} of a single A660-labeled BSA molecule at 1.5 K. The data are shown by an average (O) with a standard deviation (bar). In all measurements in the Figures, I_{VIS} was 60 W cm^{-2} and ν_{IR} was 1650 cm^{-1}.

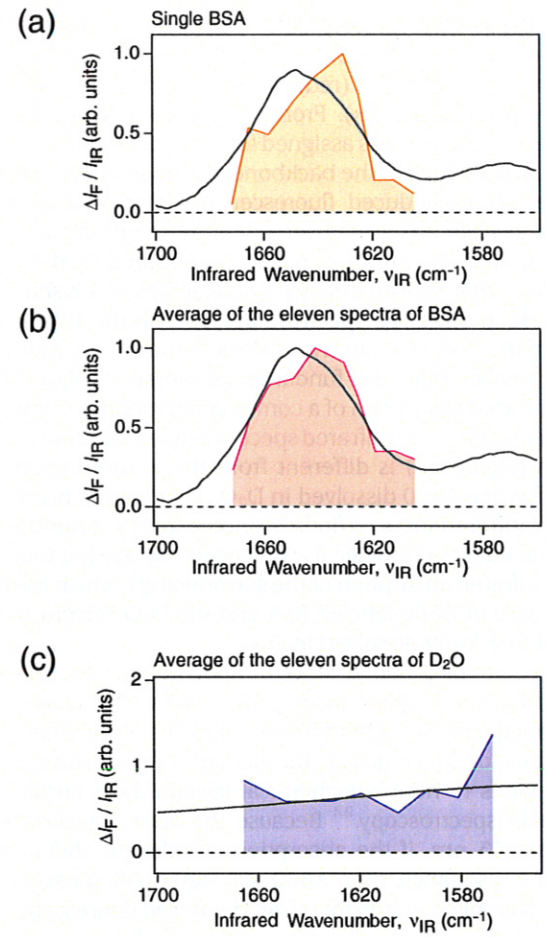

Figure 4. (a) Fluorescence-detected infrared-absorption spectrum of a single A660-labeled BSA molecule taken at 1.5 K (orange). I_{VIS} was 60 W cm^{-2} and I_{IR} was below 30 W cm^{-2}. (b) The average of the spectra taken in the same way as in part a for 11 individual A660-labeled BSA molecules (red). The black curve in parts a and b indicates the FT-IR spectrum of an ensemble of BSA. (c) The average of the 11 infrared-absorption spectra of D_2O solvent detected as infrared-induced visible-fluorescence recovery of single A660 isolated in a D_2O buffer taken at 1.5 K (blue). I_{VIS} was 110 W cm^{-2} and I_{IR} was 100 W cm^{-2}. The FT-IR spectrum of the bulk D_2O is indicated by the black curve.

kelvins. With typical intensity of the visible I_{VIS} of 60 W cm^{-2}, the time needed for individual molecules to stop fluorescing ranged from within a second to several minutes. Within 10 s on additional infrared irradiation with the intensity I_{IR} of 3000 W cm^{-2}, 70% of the molecules that had stopped fluorescing (34 out of 50) started to emit fluorescence. The remainder did not recover fluorescence with additional infrared irradiation.

The time needed for A660 to recover fluorescence depended on the intensity of the infrared I_{IR}. Time courses of fluorescence in Figure 3a show the response of a single A660-labeled BSA molecule at two different infrared intensities. The background of 60 s^{-1} was subtracted from the detected number of photons (per second) before being presented as fluorescence intensity, I_F. With I_{IR} of 30 W cm^{-2}, it took a few seconds to return to the fluorescent state. During infrared irradiation of 10 s, the molecule repeated several times a cycle between fluorescent and nonfluorescent states. When I_{IR} was raised to 400 W cm^{-2}, the fluorescence recovery became almost instantaneous. The molecule practically continued to fluoresce during the time when the infrared was on. The effect of the infrared on fluorescence was saturated at this intensity of the infrared.

We quantified the infrared-induced fluorescence recovery, ΔI_F, by measuring the fluorescence intensity averaged over 10 s after infrared irradiation was added to a nonfluorescent dye-labeled protein. Figure 3b plots ΔI_F measured for a single A660-labeled BSA molecule at 1.5 K as a function of I_{IR}, both on a logarithmic scale. The infrared wavenumber ν_{IR} was fixed at 1650 cm^{-1}. Under conditions of the weakest I_{IR} among tested, ΔI_F does have a positive correlation with I_{IR}, as suggested by a straight line of slope 1. As indicated by a broken line, ΔI_F is saturated above I_{IR} of ~300 W cm^{-2} in accordance with the saturated response in Figure 3a with I_{IR} of 400 W cm^{-2}.

We obtained the infrared absorption spectrum of a single BSA molecule by measuring the infrared-induced fluorescence recovery ΔI_F of a single A660-labeled BSA molecule as a function of ν_{IR} at 1.5 K. The result is plotted in Figure 4a in orange. The intensity of the infrared I_{IR} was kept below 30 W cm^{-2} to avoid saturation. The spectrum was measured for 11 different single A660-labeled BSA molecules, and their average is shown in Figure 4b in red. The black curve in Figure 4a,b

DOI: 10.1021/jz100858b | J. Phys. Chem. Lett. 2010, 1, 2541–2545

shows the Fourier transform infrared absorption (FT-IR) spectrum of an ensemble of BSA. In Figure 4b, the average spectrum of single BSAs (red) agrees with the FT-IR spectrum of the ensemble (black). From the agreement, the orange spectrum in Figure 4a is assigned to the C=O vibrations of the α-helical structures of the backbone of a single BSA molecule.

The infrared-induced fluorescence recovery of a single A660 molecule was also observed for free A660 dissolved in a D_2O buffer. The infrared spectrum measured by the same method as that applied to single A660-labeled BSA is shown in Figure 4c in blue. The spectrum agrees with the FT-IR spectrum of the bulk D_2O shown in black in the Figure. Although much weaker than the fundamental vibrations, D_2O does have infrared absorption of a combination mode in this wavenumber range.[21] The infrared spectrum taken for A660 bound to BSA (Figure 4b) is different from the infrared spectrum taken for free A660 dissolved in D_2O (Figure 4c). This shows that the infrared-induced fluorescence recovery of A660 is not determined by intramolecular process of the dye but induced by the infrared absorption of the surroundings, which are BSA in the case of A660-labeled BSA and the D_2O solvent in the case of free A660 dissolved in D_2O.

As for stopping fluorescence of A660 at a few kelvins, it is most probably a light-induced shift of the visible absorption wavelength due to light-induced conformational change of the protein or D_2O matrix in the vicinity of A660. The process corresponds to nonphotochemical spectral hole burning in ensemble spectroscopy.[22] Because the laser wavelength is fixed at 633 nm, if the absorption wavelength shifts away from the resonance, then A660 will stay nonfluorescent for ever. A possible scenario for infrared-induced fluorescence recovery is conformational rearrangement of the environment in the vicinity of A660 induced by absorption of infrared energy by the surroundings. To understand the mechanism of the fluorescence recovery of A660, experiments using a laser tunable in visible wavelength need to be conducted to investigate spectral diffusion of single molecules as well as spectral hole burning of an ensemble.[22,23] The results would provide the guidelines for searching for other suitable dyes.

In the present work, we developed a novel method for vibrational infrared spectroscopy of single proteins, that is, detecting the infrared-induced recovery of the visible fluorescence from a dye with which the protein was labeled. Thanks to the infrared-induced fluorescence recovery of the dye, Alexa Fluor 660, the sensitivity of detecting infrared absorption of proteins is raised to the level of visible-fluorescence detection of single molecules.

AUTHOR INFORMATION

Corresponding Author:

*To whom correspondence should be addressed. E-mail: fujiyoshi@phys.titech.ac.jp (S.F.); matsushita@phys.titech.ac.jp (M.M.).

ACKNOWLEDGMENT We thank Hirotsugu Hiramatsu, Tadamasa Shida, and Masahiro Kotani for helpful discussion and comments. We thank Sankyo Optics Industry for carving out the reflecting objectives. This work was financially supported by Grant-in-Aids for Scientific Research (19685001, 19056011, 21655055, and 18077003).

REFERENCES

(1) Orrit, M.; Bernard, J. Single Pentacene Molecules Detected by Fluorescence Excitation in a *p*-Terphenyl Crystal. *Phys. Rev. Lett.* **1990,** *65*, 2716–2719.

(2) Ambrose, W. P.; Moerner, W. E. Fluorescence Spectroscopy and Spectral Diffusion of Single Impurity Molecules in a Crystal. *Nature* **1991,** *349*, 225–227.

(3) Schmidt, T.; Schutz, G. J.; Baumgartner, W.; Gruber, H. J.; Schindler, H. Imaging of Single Molecule Diffusion. *Proc. Natl. Acad. Sci. U.S.A.* **1996,** *93*, 2926–2929.

(4) Sako, Y.; Minoghchi, S.; Yanagida, T. Single-Molecule Imaging of EGFR Signalling on the Surface of Living Cells. *Nat. Cell Biol.* **2000,** *2*, 168–172.

(5) Michalet, X.; Pinaud, F. F.; Bentolila, L. A.; Tsay, J. M.; Doose, S.; Li, J. J.; Sundaresan, G.; Wu, A. M.; Gambhir, S. S.; Weiss, S. Quantum Dots for Live Cells, In Vivo Imaging, and Diagnostics. *Science* **2005,** *307*, 538–544.

(6) Dickson, R. M.; Cubitt, A. B.; Tsien, R. Y.; Moerner, W. E. On/Off Blinking and Switching Behaviour of Single Molecules of Green Fluorescent Protein. *Nature* **1997,** *388*, 355–358.

(7) Lu, H. P.; Xun, L. Y.; Xie, X. S. Single-Molecule Enzymatic Dynamics. *Science* **1998,** *282*, 1877–1882.

(8) van Oijen, A. M.; Ketelaars, M.; Köhler, J.; Aartsma, T. J.; Schmidt, J. Unraveling the Electronic Structure of Individual Photosynthetic Pigment-Protein Complexes. *Science* **1999,** *285*, 400–402.

(9) Cogdell, R. J.; Gall, A.; Köhler, J. The Architecture and Function of the Light-Harvesting Apparatus of Purple Bacteria: From Single Molecules to *In Vivo* Membranes. *Q. Rev. Biophys.* **2006,** *39*, 227–324.

(10) Oikawa, H.; Fujiyoshi, S.; Dewa, T.; Nango, M.; Matsushita, M. How Deep Is the Potential Well Confining a Protein in a Specific Conformation? A Single-Molecule Study on Temperature Dependence of Conformational Change between 5 and 18 K. *J. Am. Chem. Soc.* **2008,** *130*, 4580–4581.

(11) Kinoshita, M.; Kamagata, K.; Maeda, A.; Goto, Y.; Komatsuzaki, T.; Takahashi, S. Development of a Technique for the Investigation of Folding Dynamics of Single Proteins for Extended Time Periods. *Proc. Natl. Acad. Sci. U.S.A.* **2007,** *104*, 10453–10458.

(12) Dong, A.; Huang, P.; Caughey, W. S. Protein Secondary Structures in Water from Second-Derivative Amide-I Infrared Spectra. *Biochemistry* **1990,** *29*, 3303–3308.

(13) Maeda, A.; Kandori, H.; Yamazaki, Y.; Nishimura, S.; Hatanaka, M.; Chon, Y. S.; Sasaki, J.; Needleman, R.; Lanyi, J. K. Intramembrane Signaling Mediated by Hydrogen-Bonding of Water and Carboxyl Groups in Bacteriorhodopsin and Rhodopsin. *J. Biochem.* **1997,** *121*, 399–406.

(14) Hiramatsu, H.; Goto, Y.; Naiki, H.; Kitagawa, T. Core Structure of Amyloid Fibril Proposed from IR-Microscope Linear Dichroism. *J. Am. Chem. Soc.* **2004,** *126*, 3008–3009.

(15) Hiramatsu, H.; Goto, Y.; Naiki, H.; Kitagawa, T. Structural Model of the Amyloid Fibril Formed by β_2-Microglobulin #21−31 Fragment Based on Vibrational Spectroscopy. *J. Am. Chem. Soc.* **2005,** *127*, 7988–7989.

(16) Zondervan, R.; Kulzer, F.; Kol'chenko, M. A.; Oritt, M. Photobleaching of Rhodamine 6G in Poly(vinyl alchol) at the Ensemble and Single-Molecule Levels. *J. Phys. Chem. A* **2004,** *108*, 1657–1665.

(17) Fujiyoshi, S.; Fujiwara, M.; Matsushita, M. Visible Fluorescence Spectroscopy of Single Proteins at Liquid-Helium Temperature. *Phys. Rev. Lett.* **2008,** *100*, 168101.

(18) Fujiyoshi, S.; Fujiwara, M.; Kim, C.; Matsushita, M.; van Oijen, A. M.; Schmidt, J. Single-Component Reflecting Objective for

Low-Temperature Spectroscopy in the Entire Visible Region. *Appl. Phys. Lett.* **2007,** *91*, 051125.
(19) Fujiwara, M.; Fujiyoshi, S.; Matsushita, M. Single-Component Reflecting Objective for Ultraviolet Imaging and Spectroscopy at Cryogenic Temperature. *J. Opt. Soc. Am. B* **2009,** *26*, 1395–1399.
(20) Hirayama, K.; Akashi, S.; Furuya, M.; Fukuhara, K. Rapid Conformation and Revision of the Primary Structure of Bovine Serum-Albumin by ESIMS and frit-FAB LC/MS. *Biochem. Biophys. Res. Commun.* **1990,** *173*, 639–646.
(21) Walrafen, G. E. Raman Spectral Studies of Water Structure. *J. Chem. Phys.* **1964,** *40*, 3249–3256.
(22) Jankowiak, R.; Hayes, J. M.; Small, G. J. Spectral Hole-Burning Spectroscopy in Amorphous Molecular-Solids and Protein. *Chem. Rev.* **1993,** *93*, 1471–1502.
(23) Hofmann, C.; Aartsma, T. J.; Michel, H.; Kohler, J. Direct Observation of Tiers in the Energy Landscape of a Chromoprotein: A Single-Molecule Study. *Proc. Natl. Acad. Sci. U.S.A.* **2003,** *100*, 15534–15538.

DOI: 10.1021/jz100858b | *J. Phys. Chem. Lett.* **2010,** *1*, 2541–2545